Reprinted from Applied Optics, Vol. 26, page 2836, July 15, 1987

Guided-wave reflectometry with micrometer resolution

B. L. Danielson and C. D. Whittenberg

We describe a new type of optical reflectometry which is useful in testing single-mode lightguide systems. This technique uses a scanning Michelson interferometer in conjunction with a broadband illuminating source and cross-correlation detection. High resolution is achieved through the limited coherence of the backscattered radiation. With this approach it is possible to distinguish scattering centers separated by only a few micrometers. In some cases loss may be estimated for components in the transmission path of a test lightguide. The basic principles of this diagnostic technique, along with some performance characteristics, are illustrated for an all-fiber reflectometer. We also discuss several laboratory applications which serve to demonstrate the resolution capabilities of this measurement concept.

I. Introduction

The development of optical signal-processing techniques in lightwave networks is now an active field of research. Some of the components required for these transparent systems are phase and amplitude modulators, optical switches, power splitters and combiners, optical amplifiers, and polarization controllers. At the present state of technology, the interconnection of these bulk-optic devices is most expeditiously done with single-mode optical fibers. As an ultimate goal, however, it would be desirable to implement these control functions on a single semiconductor chip. Fabrication techniques in this case could include planar lithographic waveguide processes analogous to those used in the familiar electrical integrated-circuit structures.

This paper describes a novel test method which can support and evaluate this microoptic technology and probe the transmission properties of other small-scale photonic systems. The technique uses a Michelson interferometer along with a low coherence source to resolve multiple discontinuities along a guided-wave structure. Discrete reflections can be located, their magnitudes measured, and, in certain conditions, attenuation of individual components estimated. The resolution is nominally a few micrometers, but in some cases it is possible to observe in the reflecting signal structure on a scale even less than one wavelength of light. We describe the properties of this time-domain reflectometer, demonstrate some performance capabilities, and illustrate its applications to several measurement problems.

II. Background

Nondestructive measurement of some optical transmission property as a function of distance along the device under test generally requires the methods of reflectometry. Diagnostics for concatenated components or long optical fiber transmission lines are usually conducted with some variation of optical time-domain reflectometry (OTDR).[1,2] This method has proved to be of immense value in the metrology of optical transmission systems. Reported measurements include determination of fiber attenuation, break location, diameter fluctuations, splice quality, mode conversion at joints, defect identification, and microbending loss. Most of the applications are associated with testing long-distance optical telecommunication systems.

In a recent review article, Healey[3] described in some detail the various types of single-mode reflectometer developed to date. These include devices based on coherent detection and optical frequency-domain instruments. Here we only mention the basic operating principles of the simplest of these, a conventional pulsed-echo OTDR. A schematic diagram of a typical device is given in Fig. 1. With this instrument a pulse of radiation is launched into the test fiber through a directional coupler. A single port both launches the pulse into the test fiber and recovers the returned signals. These signals may be classified as reflections from discrete discontinuities and a very weak distributed Rayleigh scattering. The signals are detected in a fast optical detector, processed and displayed as a function of time (or distance) on some kind of graphics display. The recorded response is often referred to as

The authors are with U.S. National Bureau of Standards, Electromagnetic Technology Division, Boulder, Colorado 80303.
Received 23 February 1987.

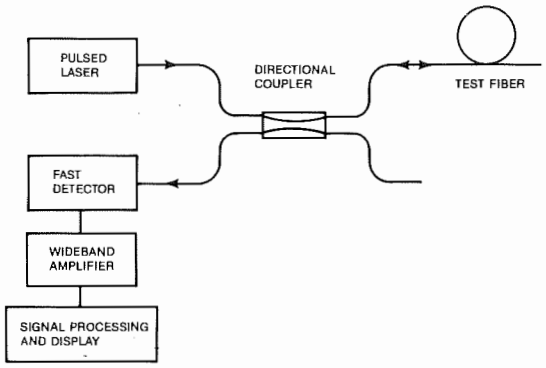

Fig. 1. Schematic diagram of a conventional pulse-echo optical time-domain reflectometer. The coupler and light transmitting elements can be made with optical fibers.

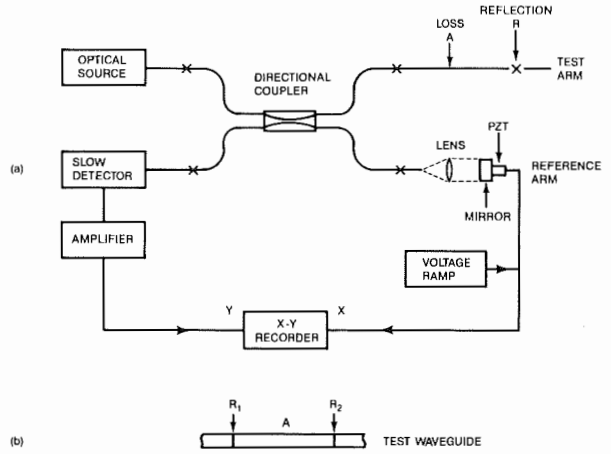

Fig. 2. Schematic diagram of the Michelson reflectometer with cross-correlation detection is depicted in (a). The location of fiber splices is indicated by X. The coupler splitting ratio is k. Interference patterns are observed from the isolated reflection R when the mirror M is scanned by the PZT. The interferogram occurs only when the difference in propagation delays between the test and reference paths is less than the coherence time of the optical source. Discrimination between different events in the test waveguide is, therefore, accomplished by the light coherence. In (b) an expanded segment of the test waveguide is shown. In some cases it is possible to estimate the loss A between the two reflections R_1 and R_2 (see text).

a signature, a term borrowed from radar usage, since it represents a unique characteristic of the system under test.

Efforts to extend these principles to high resolution reflectometry (a few centimeters or less) encounter a number of difficulties. Foremost is a bandwidth requirement on the detection electronics. The resolution is usually defined in terms of the probe pulse duration W. As the probe pulses become progressively shorter in duration, the noise accompanying these wide bandwidths ($\sim 1/W$) limits the attainable signal-to-noise ratio. Also, because of the distributed nature of Rayleigh scattering, the magnitude of the backscatter is proportional to W. This fact insures that, at the same time as system noise is increasing, the scattering signal is decreasing. Observations of Rayleigh scattering with centimeter resolution or less are, therefore, very difficult, especially immediately downstream of the more intense reflection signals. At the expense of a very limited dynamic range, conventional techniques can be used to distinguish reflections separated by only a few millimeters in an optical fiber. This is accomplished in commercial instruments using fast detectors, short-duration pulsed semiconductor lasers, and special data-processing techniques.[4]

The problems inherent in conventional time-domain reflectometry have led a number of investigators to propose entirely different methods for obtaining high resolution reflectometry. For example, centimeter resolution is possible using photon counting,[5] frequency ramped single-mode diode lasers,[6] or spatial-domain techniques.[7] The highest resolution OTDR reported to date (15 μm) has been described by Fontaine *et al.*[8] Their system used nonlinear detection in conjunction with a passively mode-locked dye laser producing pulses of 300-W peak power at 600 nm.

We now describe a very simple high resolution method in which optical coherence is the parameter which demultiplexes the myriad of signals backscattered from targets in the test waveguide.

III. Theory

A high resolution OTDR may be realized by using a Michelson interferometer as shown in Fig. 2. Radiation from a cw source with a coherence time ΔT is launched through a single-mode four-part directional coupler into both the test and reference arms of the interferometer. By translating the mirror in the reference arm, we observe reflections as a function of distance along the guided-wave structure. The detector output as a function of relative delay τ is the cross-correlation of the reflected light with the radiation returned from the reference arm. Each reflection generates an interference pattern provided that the path lengths in the two arms differ by $< c\Delta T$, where c is the velocity of light. The resulting interferograms yield information on the location and nature of the reflecting events in the lightguide. As we show, in certain cases we may also be able to infer the loss between selected targets.

This description may be quantified by considering the following somewhat simplified situation. We assume nondispersive single-mode lightguides which preserve both the state and degree of polarization. The test arm contains the discrete reflections R_i and a cumulative fractional one-way loss A_i preceding these reflections. The coupler splitting ratio K has a value between 0 and 1. A simple extension of the general interference law for stationary fields[9] allows us to express the optical power $P_d(\tau)$, which impinges on the detector from the reflection R_i as

$$P_d(\tau) = P_0 K(1-K)[1 + A_i^2 R_i + 2A_i\sqrt{R_i}|\gamma_{12}(\tau)|\cos\theta] \quad (1)$$

with

$$\theta = 2\pi f\tau + \xi. \quad (2)$$

Here P_0 is the optical power launched into the coupler, f is the mean optical frequency, and ξ is a constant phase shift. The quantity $|\gamma_{12}(\tau)|$ is the modulus of the cross-correlation function for the radiation in the two arms. The relative delay τ is given by $(x_1/v_1 - x_2/v_2)$, the difference in path lengths in the two arms divided by their respective group velocities. For simplicity we also assume no loss associated with the source, detector, and reference arms and a mirror reflectance of 1. From Eq. (1) we see that the power reaching the detector is a maximum when $K = \frac{1}{2}$ even in cases where the backscattered power is small. For these reasons we assume a 50:50 coupler in the following discussions.

The oscillating term in Eq. (1) represents the interferogram signal. The magnitude of this term is proportional to the square root of the reflectance of the target, since the interferogram originates from a term proportional to $\sqrt{(P_1P_2)}$ with P_1 and P_2 the optical power reflected from the reference and test arms, respectively. For most cases of interest in the present application, $P_2 \ll P_1$. The functional dependence of the signal response is characteristic of homodyne detection where P_1 is the local oscillator power. As R becomes very small the magnitude of the interferogram falls off much slower than would be the case for directly detected signals proportional to the first power of the reflectance.

The envelope of the interferogram generated from each reflection is $|\gamma_{12}(\tau)|$. For a quasi-monochromatic source, the width of this envelope is $\sim 1/\Delta f$ with Δf the source spectral width. Specifically, for a Gaussian spectral distribution with FWHM of Δf_{FWHM}, the interferogram is also Gaussian with a FWHM given by

$$\Delta\tau = \frac{4\ln 2}{\pi \Delta f_{\mathrm{FWHM}}}. \tag{3}$$

Visibility is an important quantity which defines the relative magnitude of the interferogram and is defined as

$$V(\tau) = \frac{P_{\max} - P_{\min}}{P_{\max} + P_{\min}}. \tag{4}$$

Under the present assumptions this becomes at the ith reflection

$$V_i(\tau) = \frac{2A_i\sqrt{R_i}}{1 + A_i^2 R_i} |\gamma_{12}(\tau)|. \tag{5}$$

From Eq. (1), we see that the visibility is independent of the magnitude of K and can have any value between 0 and 1.

The resolution of an optical reflectometer is often defined as the FWHM of a signal reflection which appears on the signature display.[10] Following this precedent, the nominal resolution Δx is approximately

$$\Delta x = \frac{v}{2\Delta f} \tag{6}$$

with v the group velocity of light. The resolution can, therefore, be controlled by choosing an optical source with a suitable frequency spectrum. The factor of 2 in Eq. (6) occurs since distance refers to one-way excursions along the test waveguide, but delay includes travel both ways. The oscillating component of the interferogram can sometimes be used to infer structure on a scale much less than that implied by Eq. (6). In fact, features due to subwavelength structure are observable. Examples of this are in Sec. III.

In Fig. 2(b) we have an expanded view of the test waveguide depicting two resolved discrete reflections, R_1 and R_2, with an intervening lossy region characterized by the fractional loss A. An examination of Eq. (1) suggests that in general we cannot simultaneously determine both the reflectance and loss from the backscattered power. However, two regimes are of special interest:

(a) R known and A estimated. If R_1 and R_2 are known, for example, at perfect Fresnel reflections, the one-way loss in decibels, $-10\log A$, may be estimated according to the relation

$$-10\log A = 5\log\left[\frac{(1-R_1)^2 R_2}{R_1}\right] + 10\left(\frac{S_1}{S_2}\right)(\mathrm{dB}). \tag{7}$$

This result follows directly from Eq. (1). Here S_1/S_2 is the ratio of the maximum amplitudes of the respective interferograms. Multiple reflections have been neglected in these relations.

(b) A negligible, R estimated. The magnitude of a reflection is of interest in several cases. High coherence sources are often sensitive to very small amounts of reflected power. The surface quality and angle at a Fresnel reflection may be of interest, and these determine backscattered power. The quality of a splice may in some cases be correlated with the signal level, although this relationship is not a clear-cut matter.[11] We can see from Eq. (5) that, if A is small, the reflectance may be estimated from the magnitude of the visibility. Also, the relative reflectance of two targets is proportional to the square root of the ratio of maximum interferogram amplitudes.

Polarization and dispersion in the interferometer can alter the shape and magnitude of the observed interferograms. Fading or reduced visibility can occur if the polarization states of the interfering beams are not identical.[12,13] Signatures can be complicated by group delay differences between the two polarization modes in a birefringent lightguide.[14] Unbalanced dispersion has the undesirable effect of not only reducing the maximum value of the visibility but broadening the interferogram as well. As long as the transmission properties are identical in the reference and test arms, no distortion of the interferogram occurs. Since chromatic dispersion is proportional to optical linewidth, signature integrity can be maintained by using higher coherence sources. Of course, this also degrades the system resolution. Dispersion compensation in the two interferometer arms is also possible. These problems are minimized in polarization-preserving silica fibers operating near the zero-dispersion wavelength of 1300 nm.

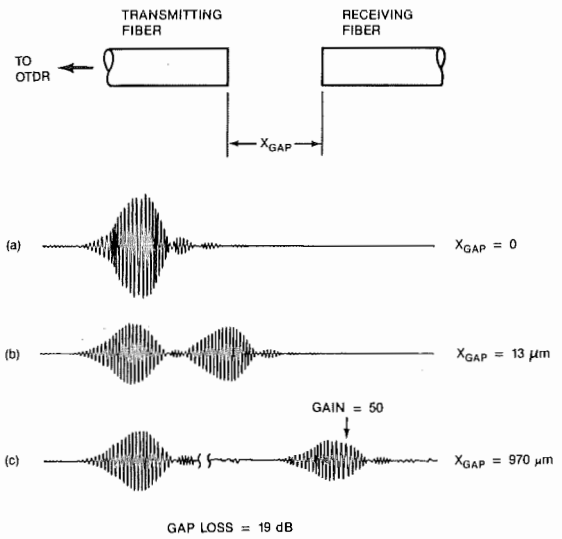

Fig. 3. Experimental interferograms generated by the Fresnel reflections at the gap between two single-mode optical fibers. In (a) the fibers are in contact, although there is still some air gap between them due to end-wedge effects. In (b) the gap is increased to ~13 μm. In (c) the separation is 970 μm. The reflected power from the receiving fiber is considerably attenuated due to diffraction effects. The scale here is multiplied by a factor of 50 relative to (a) and (b).

IV. Experiment

Our apparatus is illustrated in Fig. 2. The source was a LED operated continuously with a FWHM spectral width of ~130 nm centered at 1300 nm. This source had a multimode pigtail which was butt-coupled into the single-mode directional coupler. A maximum of 50 nW could be injected into the interferometer with this arrangement. Both arms of the interferometer consisted of 1.5-m lengths of single-mode fiber. The InGaAs detector was operated in the photovoltaic mode. Electronic filtering limited the amplified signal to a passband of ~1 Hz centered at 2 Hz. Course scanning of mirror M over a range of 7.5 cm was accomplished by means of a micrometer-driven translation stage. Fine scanning was done with a piezoelectric transducer capable of 90-μm translations. The PZT is not an ideal transducer since displacement is not a linear function of applied voltage. However, if the total voltage excursion and direction of scan are constant, the displacement vs voltage characteristic can be inferred from the fringe spacings on the X-Y recorder. A high coherence source is desirable for this distance calibration.

The minimum observable value of R, as estimated from the noise floor, was $\sim 10^{-5}$. The limiting noise was due to vibrations and dimensional instabilities.

We now describe some measurements which illustrate the capabilities of the high resolution OTDR.

A. Gap Separation

The remote measurement of the separation between two joined fibers is easily effected with this technique. This situation is illustrated in Fig. 3. The test fibers were held in vacuum chucks mounted on micromanipulators. In all cases the signatures originate from Fresnel reflections. In Figs. 3(a) and (b) the gap spacing x_{gap} can be estimated from the relation

$$x_{gap} = m\lambda/2, \tag{8}$$

where λ is the mean wavelength of the source, and m is the number of fringes. Separations of only a few micrometers are observable.

The shape of an individual interferogram can be seen in Fig. 3(b) where the reflections are clearly separated. Since the frequency spectrum of the LED is approximately Gaussian, we might expect a symmetric signature from each reflection. Instead, asymmetries and small satellites are observed. These effects may be due to unbalanced dispersion. Also, the signature is broader than that predicted from spectral width considerations. This may be accounted for by the coupler and detector wavelength dependence, which could narrow the effective spectrum.

The stability of this apparatus was insufficient to demonstrate experimentally the structure on a submicron scale. However, we have simulated this structure in Fig. 4. These interferograms are calculated summations of component reflections from the two surfaces along with their associated delays. For a zero-gap separation, the resultant return is also zero due to the π phase shift in the electric fields from the two surfaces. At an optical path difference near $\lambda/2$, the interferograms tend to interfere constructively and at λ destructively. Although the differences are slight in some cases, the interferogram at each separation is unique. Therefore, in principle at least, unambiguous spacing information can be extracted from these signatures by using appropriate deconvolution processes.

B. Loss

In Fig. 3(c) we have increased the distance x_{gap} to the point that considerable power is lost by diffraction. We can estimate the magnitude of this loss by noting that, in ideal conditions of alignment, this coupling is identical to the power coupled from the transmitting to the receiving fibers separated by a distance of $2x_{gap}$. Exact solutions to this problem have been published.[15] In our assumed conditions, the round-trip diffraction loss in decibels should be

$$\text{loss} = 10 \log[4/(G^2 + 4)] \text{ (dB)}, \tag{9}$$

where

$$G = \frac{\lambda x}{2\pi n r^2}. \tag{10}$$

Here r is the mode-field radius, and n is the fiber core index of refraction. The experimental value for the two-way gap loss, obtained from the ratio of interferogram amplitudes and Eq. (7), is within 1 dB of the calculated value of 19.4 dB using Eq. (10).

C. Stress

Externally applied stress σ in an optical fiber causes a change in pulse propagation time T according to the relation

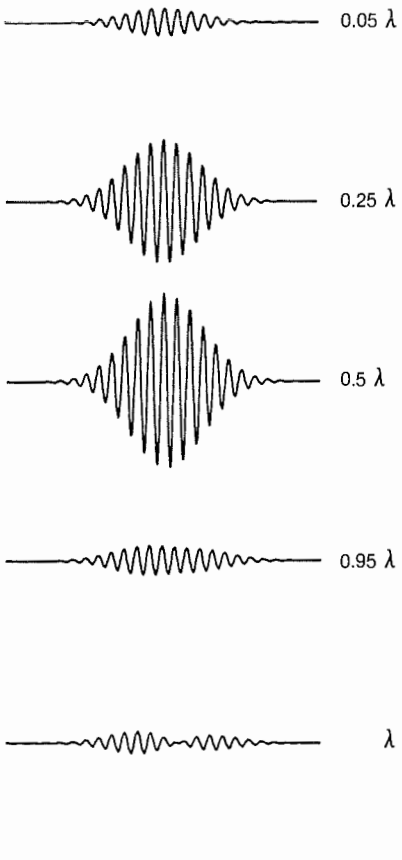

Fig. 4. Simulated interferograms for the configuration of Fig. 3. The optical path difference, twice the gap spacing, is expressed in terms of wavelengths. These signatures show that structure can be observed due to gap spacings of $<1\ \mu$m. For a zero spacing no power should be reflected. For integral multiples of λ, the signals from the two reflecting surfaces partially cancel, and at a spacing of λ/2 they reinforce each other. The responses in (a) and (d), while superficially similar, exhibit subtle shape differences.

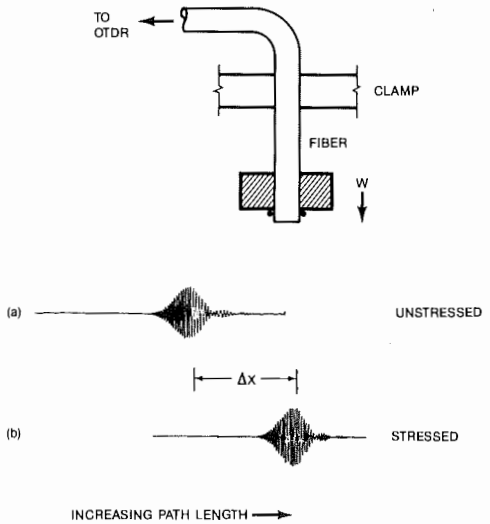

Fig. 5. Extension of a stressed fiber can be measured by observing the shift in the location of the interferogram. This was done by attaching a concentric weight W to the fiber. From this measurement we can obtain the stress-induced change in pulse propagation time.

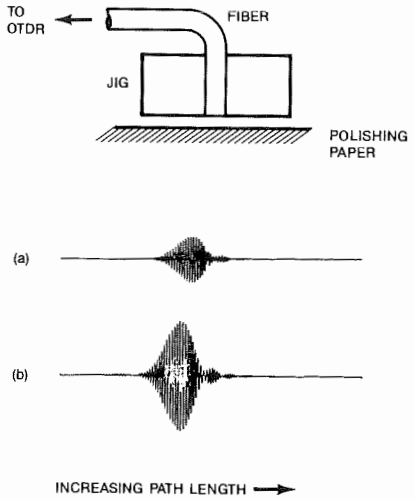

Fig. 6. Amount of material removed by polishing a fiber endface can also be estimated from the interferogram shift. The fiber is held in a jig to assure that the axis is perpendicular to the polishing surface. In (a) an as-cleaved fiber has been polished slightly on 5-μm abrasive paper. In (d) the fiber has been further finished on 1-μm abrasive paper. The quality of the endface is also indicated by the magnitude of the reflected power.

$$\frac{dT}{d\sigma} = \frac{1}{c}\left(N\frac{dL}{d\sigma} + L\frac{dN}{d\sigma}\right) \tag{11}$$

with N the group index of refraction. The total change in transit time is, therefore, due to a combination of two distinct effects.

Experimentally the combination of these effects can be determined from an arrangement depicted in Fig. 5. Here a jacketed fiber of length $L = 20$ cm was stressed by means of a mass of ~10 g. We observed a shift in the interferogram of ~28 μm measured as the sum of translations of the micrometer screw and PZT. These data are also shown in Fig. 5. The stress variation is ~60 ps/km MPa. By way of comparison, Hartog *et al.*[16] quote a value of 54 ps/km MPa for bare experimental fiber at a wavelength of 0.9 μm.

This transit-time information is required for optical-fiber strain-gauge calibration[17] and for measurement of stress in optical waveguides of known unstressed dimensions.[18]

D. Optical Polishing

Very small changes in physical length of an optical system can be observed with the high resolution OTDR. For example, we can monitor the removal of material which occurs during the polishing of a fiber end in the test arm. The physical length Δx of fiber removed may be estimated from the fringe shift according to the relation

$$\Delta x = m\lambda/2N, \tag{12}$$

where m is the number of observed fringes shifted in the interferogram after polishing.

Figure 6 illustrates the experimental arrangement. The fiber was mounted in a jig and hand polished on abrasive paper. The rough-polished reflection is compared in magnitude and position with the reflection

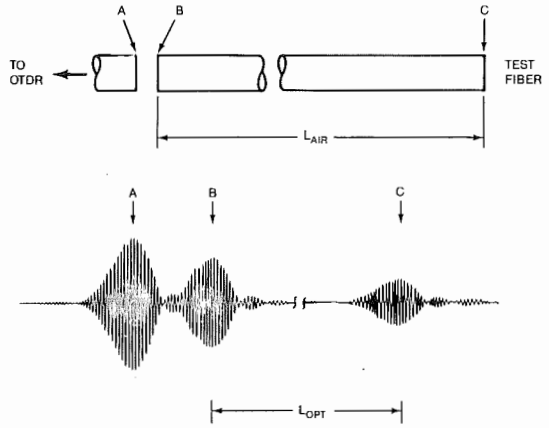

Fig. 7. Group index of refraction for a short length of single-mode fiber can be obtained from the ratio of the physical length L_{air} to the distance between appropriate reflections on the interferogram L_{opt}.

from the same end after a small amount of polishing on 1-μm grit abrasive paper. The interferogram is due to the Fresnel reflection of the fiber end. These observations were made without removing the fiber from the jig. In these measurements care must be exercised to insure that the spatial configuration of the fiber in the test arm of the interferometer is preserved as much as possible. Extraneous bends and twisting of the fiber can easily cause shifts of several fringes.

E. Group Index

The group velocity of light v, or the group index $N = c/v$, varies slightly in different optical waveguides according to specifics of manufacturing. Knowledge of this parameter is necessary for accurate length measurements using the method based on the time of flight of a short-duration optical pulse. Most commercial OTDRs have a user-operated control for adjusting the appropriate N for each test condition. Also, fiber dispersion may be obtained in a straightforward way from the dependence of the group index on wavelength.

Figure 7 illustrates a method for measuring N from short (a few centimeters) optical waveguides. The group index can be specified as

$$N = L_{air}/L_{opt}, \tag{13}$$

where L_{air} is the physical length of the fiber, and L_{opt} is the optical-path distance between the interferogram end reflections. As shown in the figure, the Fresnel reflections are suitable for this purpose. For the most accurate measurements, L_{air} can be measured interferometrically, but this was not attempted here. We estimated L_{air} by mounting a 2.5-cm length of fiber on a micropositioner and aligning alternate ends under the cross hairs of a microscope. The principal errors are associated with locating the precise position of the end of the fiber. The overall uncertainty was estimated to be <0.05%. This analysis assumes a uniform fiber, a condition which seems to be satisfied fairly well in the cases in which this property has been measured.[19]

There can be a problem associated with attempts to measure very accurately the length of a nonrigid body such as an optical fiber. Many measurement procedures tend to introduce a certain amount of stress into the fiber. This can occur when it is wound on a drum or stretched into alignment with a rule. The stress changes the dimensions of the sample. However, for lengths of a few centimeters or so, as required here, the fiber behaves as a fairly rigid body, and this problem does not arise.

V. Other Metrology Applications

A. Dispersion

We have seen that the dispersion in the two arms of the interferometer must be matched if broadening of the interferogram is to be avoided. However, there may be cases where distortion, or pulse broadening, is the effect of interest. In fact distortion as a function of distance can be measured in concatenated optical devices composed of different transmitting materials. Bomberger and Burke[20] demonstrated that interferometric techniques, similar to those described here, could be used to determine dispersion in short lengths of single-mode optical fiber. More accurate methods have been reported recently which use the Mach-Zehnder configuration.[21,22]

B. Sensors

Sensors represent an important class of applications of optical fiber technology.[23] It was realized at an early date that the OTDR can be used as a single-ended distributed sensor capable of measuring many physical quantities such as stress, fields, or temperature.[24] One transmission line can contain a large number of sensors which can be individually addressed by demultiplexing in the time domain.

Used as a sensor, the low coherence Michelson OTDR has unique properties. It allows for a perturbation to be measured to interferometric accuracies without the 2π ambiguity normally associated with interferometric sensors. That is, for time resolutions of $<1/f$, phase measurements can be used to interpolate between fringes, and the envelope of the interferogram can be used to establish which fringe is undergoing the observed phase change. Therefore, absolute changes in optical path length due to some external stimulus can be made with submicrometer precision.

VI. Summary

We have developed a new reflectometry technique which uses limited temporal coherence to distinguish between separate scattering centers occurring in small-scale lightguide structures. With a scanning Michelson interferometer and cross-correlation detection, continuous wave light with coherence time ΔT is capable of the same instrumental resolution as optical pulses with temporal duration ΔT. As an example, we have shown that a cw LED can yield a resolution equivalent to a pulse of ~60-fs duration. In some specific cases, backscatter signatures can display structure due

to discrete reflecting surfaces separated by temporal delays of <3 fs. Coherent detection with its attendant advantages is an integral part of this approach. This and modest bandwidths requirements permit observation of very small reflections. With low coherence sources (LED, white light) there need be no concern about instabilities arising from optical feedback. When compared to fast pulse reflectometry methods, these characteristics permit considerable simplification in experimental architecture.

The authors acknowledge the support of this research by the Naval Ocean Systems Center, San Diego, CA.

References

1. M. K. Barnoski, M. D. Rourke, S. M. Jensen, and R. T. Melville, "Optical Time Domain Reflectometer," Appl. Opt. **16,** 2375 (1977).
2. S. D. Personick, "Photon Probe—an Optical Time-Domain Reflectometer," Bell Syst. Tech. J. **56,** 355 (1977).
3. P. Healey, "Review of Long Wavelength Single-Mode Optical Fiber Reflectometry Techniques," IEEE/OSA J. Lightwave Technol. **LT-3,** 876 (1985).
4. "A Short Technical Note on High Resolution Optical Time-Domain Reflectometry," Opto-Electronics, Inc., Oakville, Ont. L6L 5K9 Canada.
5. G. Ripamonti and S. Cova, "Centimeter-Resolution Optical Time Domain Reflectometry using Single-Photon Avalanche Diodes," in *Technical Digest, Conference on Lasers and Electro-Optics* (Optical Society of America, Washington, DC, 1986), paper THK21.
6. D. Uttam and B. Culshaw, "Precision Time-Domain Reflectometry in Optical Fiber Systems using a Frequency Modulated Continuous Wave Ranging Technique," IEEE/OSA J. Lightwave Technol. **LT-3,** 971 (1985).
7. N. J. Frigo, A. Dandridge, and C. A. Villarruel, "An Optical Space-Domain Reflectometer Based on the Faraday Effect," IEEE/OSA J. Lightwave Technol. **LT-4,** 256 (1986).
8. J. J. Fontaine, J. C. Diels, and C. Y. Wang, "Subpicosecond-Time-Domain Reflectometry," Opt. Lett. **6,** 405 (1981).
9. M. Born and E. Wolf, *Principles of Optics* (Pergamon, New York, 1964), Chap. 10.
10. B. L. Danielson, "Optical Time-Domain Reflectometer Specifications and Performance Testing," Appl. Opt. **24,** 2313 (1985).
11. N. Kashima and I. Sankawa, "Reflection Properties of Splices in Graded-Index Optical Fibers," Appl. Opt. **22,** 3820 (1983).
12. P. Healey, "Fading Rates in Coherent OTDR," Electron. Lett. **20,** 443 (1984).
13. T. Okoshi, "Polarization-State Control Schemes for Heterodyne or Homodyne Optical Fiber Communications," IEEE/OSA J. Lightwave Technol. **LT-36,** 1232 (1985).
14. M. Monerie and F. Alard, "Birefringence and Polarization Dispersion Measurements in High-Birefringence Single-Mode Fibers," Electron. Lett. **23,** 198 (1987).
15. S. Nemoto and T. Makimoto, "Analysis of Splice Loss in Single-Mode Fibers Using a Gaussian Field Approximation," Opt. Quantum Electron. **11,** 447 (1979).
16. A. H. Hartog, A. J. Conduit, and D. N. Payne, "Variation of Pulse Delay with Stress and Temperature in Jacketed and Unjacketed Optical Fibers," Opt. Quantum Electron. **11,** 265 (1979).
17. R. Kist, S. Ramakrishnan, and H. Wolfelschneider, "The Fiber Fabry-Perot and its Application as a Fiber-Optic Sensor Element," Proc. Soc. Photo-Opt. Instrum. Eng. **586,** 126 (1985).
18. R. W. A. Ayre, "Measurement of Longitudinal Strain in Optical Fiber Cables During Installation by Cable Ploughing," IEEE/OSA J. Lightwave Technol. **LT-4,** 15 (1986).
19. F. M. Sears and L. G. Cohen, "Interferometric Measurements of Dispersion-Spectra Variations in a Single-Mode Fiber," IEEE/OSA J. Lightwave Technol. **LT-2,** 181 (1984).
20. W. D. Bomberger and J. J. Burke, "Interferometric Technique for the Determination of Dispersion in a Short Length of Single-Mode Optical Fiber," in *Technical Digest, Symposium on Optical Fiber Measurements*, Boulder, CO (1980).
21. M. J. Saunders and W. B. Gardner, "Precision Interferometric Measurement of Dispersion in Short Single-Mode Fibers," in *Technical Digest, Symposium on Optical Fiber Measurements*, Boulder, CO (1984), pp. 123–126.
22. J. Stone and L. G. Cohen, "Minimum Dispersion Spectra of Single-Mode Fibers Measured with Subpicosecond Resolution by White-Light Crosscorrelation," Electron. Lett. **18,** 716 (1982).
23. T. G. Giallorenzi, J. A. Bucaro, A. Dandridge, G. H. Sigel, Jr., J. H. Cole, S. C. Rashleigh, and R. G. Priest, "Optical Fiber Sensor Technology," IEEE J. Quantum Electron. **QE-18,** 626 (1982).
24. A. J. Rogers, "Polarization-Optical Time Domain Reflectometry: A Technique for the Measurement of Field Distributions," Appl. Opt. **20,** 1060 (1981).